


 Cite this: *RSC Adv.*, 2021, 11, 23385

 Received 26th May 2021
 Accepted 25th June 2021

DOI: 10.1039/d1ra04096k

rsc.li/rsc-advances

Nonflammable UV protective films consisting of clay and lignin with tunable light/gas transparency†

 Kazuhiro Shikinaka,^{ID}*^a Asami Suzuki^a and Yuichiro Otsuka^{ID}^b

In this paper, we present nonflammable UV protective films consisting of clay minerals and lignin derivatives. The nonflammable transparent films were produced by mixing clay with a lignin derivative extracted from plants by simultaneous enzymatic saccharification and comminution. The preparation procedure did not require hazardous chemicals. The optical properties and gas permeability of the films could be tuned by the components and phase separation structure of the clay minerals and lignin derivatives. In particular, the gas transmittance of the films could be controlled in the range of several mol m⁻² s⁻¹ Pa⁻¹. The present film uses mineral and plant components as high-value industrial materials and reduces the environmental load of extracting limited petroleum-based resources.

1 Introduction

A low-carbon society requires breaking away from oil-refinery-based industries for sustainable development.¹ As alternatives to petroleum resources, minerals and plants have potential in biomass-refinery-based industries.^{2,3} Clay minerals, which are inorganic geopolymers in soil, are the main component of mineral resources; they have various applications such as the following: cosmetics and plastic substitutes.⁴ Claist® is a functional film consisting of a platelet clay mineral and an organic polymer in which densely stacked clay platelets induce gas-barrier capacity and incombustibility.⁵ The various attractive characteristics of Claist® encouraged this assessment on its industrial applications.

Claist® consists of clay minerals and lignin derivatives, an aromatic polymer in plant, has been reported.^{6,7} Lignin consists of propenyl phenol units, which are the second-most abundant nonedible plant biomass and have potential as a renewable alternative to synthetic aromatic polymers.^{8,9} One important problem limiting the use of lignin derivatives is the necessity of hazardous chemicals for their extraction, such as pulping methods, which results in environmental degradation and the deterioration of lignin.^{10–12} To overcome this problem, we recently proposed a novel method for extracting lignin: simultaneous enzymatic saccharification and comminution (SESC). In this process, wet-type ultrafine bead milling and enzymatic reactions for plants were used to isolate polysaccharides and lignin, which are the main components of plants, as a sugar solution and lignin water dispersion without the

use of toxic reagents and the formation of byproducts.^{13,14} The obtained sugar solution and lignin water dispersion can be used in the production of methane gas/drinkable alcohol^{15,16} and for heat-proofing filler/UV absorber,^{17–21} respectively.

The lignin derivative extracted by SESC (later denoted as SESC lignin) is a water-dispersed nanoparticle.¹³ The SESC lignin forms a brown transparent film. However, this self-standing film is comprised of inhomogeneous small pieces that are too brittle to be used to manufacture some products. The Claist® fabrication technique enables the production of a SESC lignin uniform self-standing film having A4 size.²² This film was formed only from clay minerals, and SESC lignin exhibited excellent UV protection because of the chemical structure of lignin, which provides properties such as nonflammability and high moisture/gas transmittance. The characteristics of these films encouraged the utilization of mineral and plant resources as alternatives to petroleum-based materials and as novel high-value industrial materials consisting of natural components such as plants and minerals. The UV protection properties of lignin derivatives are expected to find applications as novel “green” functional polymers to help achieve sustainable development goals (SDGs) such as SDG 17.14.²³

In this study, the functionality of a film consisting of clay minerals and SESC lignin was controlled *via* structural change of the films. The gas transmittance of the films was controlled by the miscibility of the components in the films. The miscibility was tuned by the interaction between clay minerals and SESC lignin. Then, the optical properties (*i.e.*, light transmittance and haze value) and gas shielding properties were improved simultaneously by optimizing the clay species and the addition of a compatibilizer for film preparation. The tunable functionality of the films encouraged the utilization of mineral and plant-based materials for industrial applications such as gas-transmittance-controlled transparent UV protective films.

^aResearch Institute for Chemical Process Technology, National Institute of Advanced Industrial Science and Technology, Nigatake, 4-2-1, Miyagino-ku, Sendai 983-8551, Japan. E-mail: kaz.shikinaka@aist.go.jp

^bForestry and Forest Products Research Institute, Matsunosato, 1, Tsukuba 305-8687, Japan

† Electronic supplementary information (ESI) available. See DOI: 10.1039/d1ra04096k



2 Materials and methods

2.1 Materials

Ultrapure water (Milli-Q® Advantage A10® system, Millipore™, Eschborn, Germany) was used throughout the study. Clay minerals, Li⁺ montmorillonite (MMT; Kunipia M by Kunimine Industries Co., Ltd, Japan), and Li⁺ stevensite (ST; section-SA by Kunimine Industries Co., Ltd, Japan) were used as received. Epocros® (WS-700, $M_w = 4 \times 10^4$) and poly(vinyl alcohol) ($M_n = 2 \times 10^3$) were purchased from Nippon Shokubai Co. Ltd and Nacalai Tesque inc., respectively. The other reagent-grade chemicals were purchased from Tokyo Chemical Industry Co., Ltd and DuPont™ Genencor® Science and used without further purification. SESC lignin was prepared from Japanese cedar according to the basic procedures described as follows.^{13–22}

For SESC treatment, a mixture of cedar powder (10 w/w% for water; 0.01–2 mm ϕ), an enzyme cocktail prepared by combining equal amounts of commercial enzymes OPTIMASH XL containing cellulase and xylanase (10 300 U g⁻¹) and OPTIMASH BG containing xylanase and β -glucosidase (6200 U g⁻¹) from DuPont™ Genencor® Science, and 100 mM phosphate buffer (pH 6.0) were ground by bead milling (Labstar® LMZ015; Ashizawa Finetech Ltd, Japan) at a peripheral velocity of 14.0 m s⁻¹ at 50 °C. Stainless steel inactivates the enzyme. Therefore, the inner walls of the LMZ015 vessel were covered with a ceramic lining to prevent damage to the enzyme. Following bead milling for 2 h using 0.5 mm ϕ zirconia beads, the obtained mixture was centrifuged at 10 000 $\times g$ for 30 min. The saccharide-containing supernatant was then collected, and the precipitate was milled once more under the same enzyme and buffer conditions using 0.1 mm ϕ zirconia beads. The final slurry was centrifuged at 10 000 $\times g$ for 30 min. The resulting supernatant was recovered. The lignin-rich precipitate (SESC lignin) was washed twice by mixing with an equal amount of ultrapure water before centrifugation under the aforementioned conditions.

2.2 Preparation of films consisting of clay and SESC lignin

The films consisting of clay and SESC lignin were prepared in the following manner: a certain amount of clay hydrogel was dispersed in ultrapure water in a homogenizer operated at 6000 rpm for 15 min. The SESC lignin water dispersion at a certain concentration was dropped into the clay dispersion with stirring. Epocros® or poly(vinyl alcohol) were also added as required to change the structure of the films or to reinforce the films, respectively. Stirring was continued for 25 min. The stirred mixture was cooled at room temperature for 30 min and then mixed at 2000 rpm for 5 min using a planetary centrifugal mixer (ARE-250 Thinly Co., Ltd, Japan). Finally, the mixture was passed through a sieve with a 53 μ m mesh and degassed at 2200 rpm for 10 min, again using a planetary centrifugal mixer. The resulting gel-like mixture was cast onto a polyethylene terephthalate (PET) sheet using a film-casting knife (clearance gap 0.6 mm) and dried under ambient conditions for approximately one day. The dried self-standing films were removed

from the PET sheet, thus yielding approximately 0.02 mm thick film products. The films consisting of MMT were heat annealed to give a waterproof character.²²

2.3 Structural estimation of the films

The structural observations and elemental mapping of the cross-sections of the film were performed using a high-resolution field-emission transmission electron microscope (FE-TEM, JEOL JEM 2100F) operating at 200 kV.

2.4 Measurement of gas transmittance properties

The helium gas transmission rates (HTR) and oxygen gas transmission rates (OTR) were measured using a gas transmission testing system based on gas chromatography and the differential pressure method (GTR-10XASS, GTR Tec Corporation). The temperature, differential pressure, and measurement time were 311.7 K, 241.3 kPa, and 72 h, respectively.

2.5 Measurement of the optical properties

The total light transmittance (TLT) and haze values were measured using a haze meter (NDH5000, Nippon Denshoku Ind. Co., Ltd, Japan). The transmittance at 200–800 nm was estimated using a UV-vis spectrophotometer (U-2910, Hitachi High-Technologies, Co., Japan). The average UVA and UVB transmittances were estimated within the 315–400 and 290–315 nm ranges, respectively, according to AS/NZS4399.

2.6 Measurement of thermal properties

The flame retardance was estimated using the vertical burning test according to the UL-94 vertical method following the ISO 1210 protocol.

3 Results and discussion

3.1 Control of the gas permeability of the films from natural clay and lignin

A previous study reported that water-dispersed mixtures of clay and SESC lignin provide transparent films that have a UV protective and noncombustible nature (later denoted as clay–lignin film) after drying.²² The self-standing clay–lignin films consisting of natural clay (MMT) and SESC lignin have two separated phases. As shown in Fig. 1, these phases in the clay–

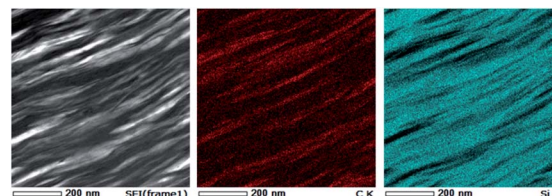


Fig. 1 Typical transmission electron microscopy (TEM) image (left), silicon mapping (middle), carbon mapping (right) of clay–lignin film consisting of MMT and SESC lignin (MMT : SESC lignin = 8 : 2 w/w%). The carbon- and silicon-rich region consisted mainly of SESC lignin and MMT, respectively.

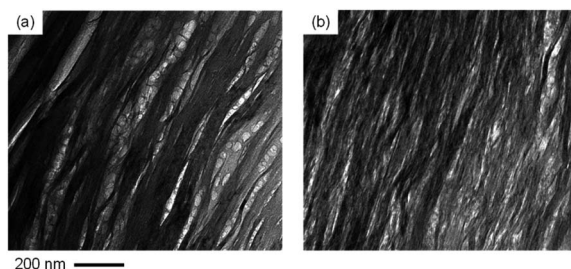


Fig. 2 Typical high-magnified TEM image of clay–lignin films consisting of MMT and SESC lignin without (a, MMT : SESC lignin = 8 : 2 w/w%) or with Epocros® (b, MMT : SESC lignin : Epocros® = 7 : 2 : 1 w/w%).

lignin film mainly consist of carbon or silicon atoms. Thus, SESC lignin and MMT in the clay–lignin film showed phase separation. The SESC lignin did not intercalate into the MMT interlayers,²² which induces clear phase separation of SESC lignin and MMT.

The SESC lignin-rich phases (a carbon-rich region in Fig. 1) have a porous structure (Fig. 2a), and the SESC lignin never intercalated into MMT interlayers (Fig. S1†) that induce the high gas/moisture transmittance nature of the clay–lignin films, *i.e.*, the HTR and OTR of the clay–lignin film consisting of MMT and SESC lignin are 4.4×10^{-18} and 5.0×10^{-17} mol m m⁻² s⁻¹ Pa⁻¹.²² The gas permeability of clay–lignin films was controlled *via* their phase structure. A polyacrylate equipped with oxazoline groups (Epocros®) interacts with clay (*via* intercalation) and lignin derivatives (*via* covalent bonding between the oxazoline group of Epocros® and hydroxyl group of lignin) as reported elsewhere.⁷ Because of these characteristics, Epocros® simultaneously intercalated into the MMT interlayer (Fig. S1†) and crosslinked with SESC lignin (Fig. S2†). Therefore, the mixing of Epocros® in the clay–lignin films makes a uniform distribution of clay and lignin (Fig. 2b). By changing the phase structure and intercalation of polymer into the MMT interlayer, the HTR of the clay–lignin film decreased from 4.4 to 1.6×10^{-18} mol m m⁻² s⁻¹ Pa⁻¹. Thus, the gas permeability of the clay–lignin film can be tuned by its structural change. The light transmittance and turbidity of the clay–lignin films were never

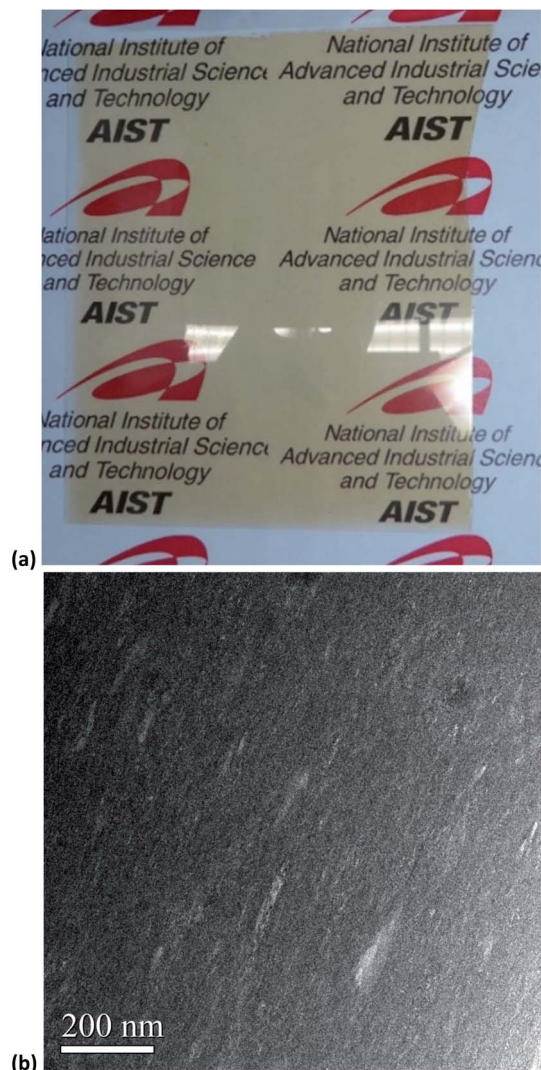


Fig. 3 (a) Photograph and (b) TEM image of typical clay–lignin coated film on PET surface consisting of ST and SESC lignin (ST : SESC lignin = 8 : 2 w/w%). The size of film is approx. A4-paper size.

changed by the addition of Epocros®, as shown in Table 1. The phase structure in the clay–lignin films did not affect their optical nature.

Table 1 Physical properties of the clay–lignin films

Clay/polymer	OTR [mol m m ⁻² s ⁻¹ Pa ⁻¹]	HTR [mol m m ⁻² s ⁻¹ Pa ⁻¹]	Annealing condition	
MMT/non ⁷	5.0×10^{-17}	4.4×10^{-18}	150 °C, 24 h	
MMT/Epocros	N. D.	1.6×10^{-18}	110 °C, 72 h	
ST/non	N. D.	74×10^{-18a}	No annealing	
ST/PVA	$<4.0 \times 10^{-20a}$	0.51×10^{-18a}	No annealing	
Clay/polymer	TLT [%]	Haze [%]	UVA [%]	UVB [%]
MMT/non ⁷	56	41	2.0	0
MMT/Epocros	54	58	2.0	0
ST/non ^a	79	3.9	6.9	0
ST/PVA	85	5.2	21	1.5

^a Measured for coated films on a PET substitute.

3.2 Improvement of optical properties in the clay–lignin films

The TLT and haze value for the clay–lignin film consisting of MMT and SESC lignin was 56 and 41%, there are lower and higher value than ordinary polymer films, respectively. To overcome this problem, clay species in the clay–lignin films changed from natural clay (*i.e.*, MMT) to synthetic clay, which gives a higher transparent coating film relative to natural clay because of the difference in its particle size.²⁴ The clay–lignin films consisting of Li⁺ stevensite (ST), a synthetic clay, and SESC lignin (Fig. 3a) showed a high TLT (79%) and low haze value (3.9%) at the same time exhibiting a UV protective nature, *i.e.*, UVA and UVB transmittance were 6.9 and 0%, respectively (Fig. S3† and Table 1). The HTR of the film was higher ($74 \times 10^{-18} \text{ mol m}^{-2} \text{ s}^{-1} \text{ Pa}^{-1}$) than that of the clay–lignin film consisting of MMT and SESC lignin. As shown in Fig. S1,† the SESC lignin was never inserted into the clay interlayers. This tendency induced poor gas barrier properties of the clay–lignin films consisting of ST and SESC lignin, even a uniform dispersion of clay and SESC lignin in the clay–lignin film (Fig. 3b), because of gaps between clay platelets. Thus, the optical properties can be improved by changing the clay species. On the other hand, the clay–lignin film consisting of ST and SESC lignin was too brittle to treat as a self-standing film and exhibited poor gas barrier properties.

3.3 Self-standing clay–lignin film with good optical properties and gas permeability

The inclusion of PVA as a compatibilizer gives the self-standing nature to the clay–lignin film consisting of ST and SESC lignin

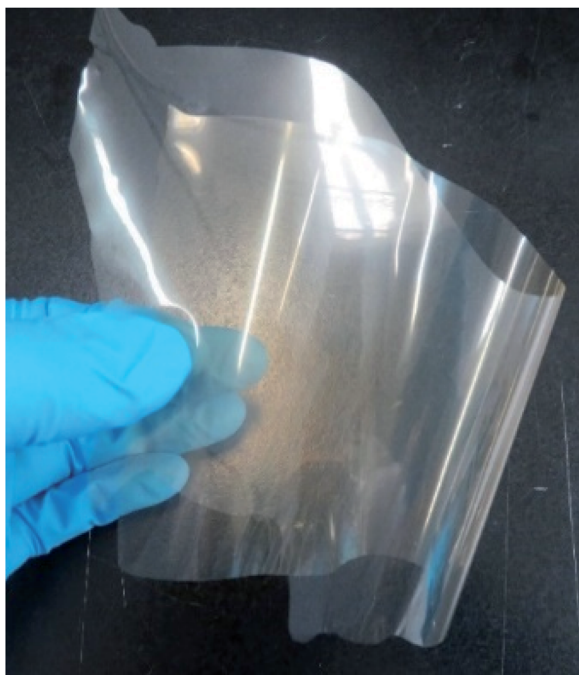


Fig. 4 Photograph of a self-standing clay–lignin film consisting of ST, PVA and SESC lignin (ST : PVA : SESC lignin = 76 : 19 : 5 w/w%). The size of film is approx. A4-paper size.

(Fig. 4). The self-standing films also exhibited a high TLT (85%) and low haze value (5.2%). As shown in Table 1, the UVA and UVB transmittance was also improved by the addition of 5 w/w% SESC lignin relative to neat ST and PVA films (*e.g.*, the UVA and UVB transmittance of the films consisting of ST and PVA (ST : PVA = 80 : 20) were 88 and 86%, respectively). The rank of the flame retardant grade in the UL94 standard of this clay–lignin film was V-0, similar to ordinary engineering plastics (*e.g.*, the fluorocarbons and poly(vinyl chloride)) and the clay–lignin films consisting of MMT/ST and SESC lignin.²² The film showed an excellent gas shielding nature (HTR: $0.51 \times 10^{-18} \text{ mol m}^{-2} \text{ s}^{-1} \text{ Pa}^{-1}$, OTR: $<4.0 \times 10^{-20} \text{ mol m}^{-2} \text{ s}^{-1} \text{ Pa}^{-1}$) compared to other clay–lignin films.^{7,22} In particular, the OTR of this clay–lignin film was lower than that of the oxygen gas barrier films reported elsewhere.^{25–28} The PVA intercalated into the clay interlayer in the film (Fig. S4†) and induced the high gas shielding nature of clay–lignin film because of shielding pores between the clay platelets.

4 Conclusions

Nonflammable UV protective films consisting of clay and lignin were prepared. The function of the films, such as the optical properties and gas transmittance, could be controlled by changing the film structure through optimization of the film components. In particular, gas transmittance of the films for He and O₂ gas could be controlled in the range of several $\text{mol m}^{-2} \text{ s}^{-1} \text{ Pa}^{-1}$, *i.e.*, the OTR of the clay–lignin film was a maximum of three orders of magnitude lower than poly(ethylene terephthalate) films ($2.0 \times 10^{-17} \text{ mol m}^{-2} \text{ s}^{-1} \text{ Pa}^{-1}$).²⁹

The films could be prepared using an environmentally friendly process, *i.e.*, by purification, mixing, and drying of clay mineral, lignin, and compatibilizer (as needed) in water, without hazardous chemicals. The resulting films exhibited various functions, such as UV protection and tunable gas transmittance nature with incombustibility. The film production described in this paper encourages the use of mineral and plant components as high-value industrial materials (*e.g.*, nonflammable UV protection transparent films with controllable gas transmittance nature). Furthermore, the use of mineral and plant components reduces the environmental load of extracting limited petroleum-based resources.

Author contributions

Kazuhiro Shikinaka: methodology, formal analysis, validation, conceptualization, funding acquisition, project administration, writing – original draft. Asami Suzuki: data curation, investigation, methodology, formal analysis, writing – original draft. Yuichiro Otsuka: project administration, resources, writing – review & editing.

Conflicts of interest

There are no conflicts to declare.

Acknowledgements

This study was supported by a grant from JST ALCA Grant Number JPMJAL1601 and JST-Mirai R&D Grant Number JPMJMI19E8. The authors would like to thank Enago (<http://www.enago.jp>) for the English language review.

Notes and references

- 1 B. Kamm, P. R. Gruber and M. Kamm, *Biorefineries-Industrial Processes and Products*, Wiley-VCH, Weinheim, Germany, 2006.
- 2 A. J. Ragauskas, C. K. Williams, B. H. Davison, G. Britovsek, J. Cairney, C. A. Eckert, W. J. Frederick Jr, J. P. Hallett, D. J. Leak, C. L. Liotta, J. R. Mielenz, R. Murphy, R. Templer and T. Tschaplinski, *Science*, 2006, **311**, 484.
- 3 H. H. Murray, *Clay Miner.*, 1999, **34**, 39.
- 4 M. Stöter, S. Rosenfeldt and J. Breu, *Annu. Rev. Mater. Res.*, 2015, **45**, 129.
- 5 T. Ebina and F. Mizutani, *Adv. Mater.*, 2007, **19**, 2450.
- 6 K. Takahashi, R. Ishii, T. Nakamura, A. Suzuki, T. Ebina, M. Yoshida, M. Kubota, T. T. Nge and T. Yamada, *Adv. Mater.*, 2017, **29**, 1606512.
- 7 A. Suzuki, K. Shikinaka, R. Ishii, H. Yoshida, T. Ebina, T. Ishida, T. T. Nge and T. Yamada, *Appl. Clay Sci.*, 2019, **180**, 105189.
- 8 *Lignin: Occurrence, Formation, Structure and Reactions*, ed. K. V. Sarkanen, C. H. Ludwig, K. V. Sarkanen and C. H. Ludwig, Wiley Interscience, New York, 1971.
- 9 H. Wang, Y. Pu, A. Ragauskas and B. Yang, *Bioresour. Technol.*, 2019, **271**, 449.
- 10 E. Adler, *Wood Sci. Technol.*, 1977, **11**, 169.
- 11 S. Aziz and K. V. Sarkanen, *Tappi J.*, 1989, **72**, 169.
- 12 K. Shikinaka, N. Fujii, S. Egashira, Y. Murakami, M. Nakamura, Y. Otsuka, S. Ohara and K. Shigehara, *Green Chem.*, 2010, **12**, 1914.
- 13 K. Shikinaka, Y. Otsuka, R. R. Navarro, M. Nakamura, T. Shimokawa, M. Nojiri, R. Tanigawa and K. Shigehara, *Green Chem.*, 2016, **18**, 5962.
- 14 R. R. Navarro, Y. Otsuka, M. Nojiri, S. Ishizuka, M. Nakamura, K. Shikinaka, K. Matsuo, K. Sasaki, K. Sasaki, K. Kimbara, Y. Nakashimada and J. Kato, *BMC Biotechnol.*, 2018, **18**, 79.
- 15 R. R. Navarro, Y. Otsuka, K. Matsuo, K. Sasaki, K. Sasaki, T. Hori, H. Habe, M. Nakamura, Y. Nakashimada, K. Kimbara and J. Kato, *Bioresour. Technol.*, 2020, **300**, 122622.
- 16 Y. Otsuka, M. Nojiri, N. Kusumoto, R. R. Navarro, K. Hashida and N. Matsui, *RSC Adv.*, 2020, **10**, 39753.
- 17 K. Shikinaka, H. Sotome, Y. Kubota, Y. Tominaga, M. Nakamura, R. R. Navarro and Y. Otsuka, *J. Mater. Chem. A*, 2018, **6**, 837.
- 18 H. Sotome, K. Shikinaka, A. Tsukidate, Y. Tominaga, M. Nakamura and Y. Otsuka, *Polym. Degrad. Stab.*, 2020, **179**, 109273.
- 19 K. Shikinaka, A. Tsukidate, Y. Tominaga, H. Inoue and Y. Otsuka, *Polym. J.*, 2021, DOI: 10.1038/s41428-021-00473-3.
- 20 K. Shikinaka, M. Nakamura and Y. Otsuka, *Polymer*, 2020, **190**, 122254.
- 21 K. Shikinaka, M. Nakamura, R. R. Navarro and Y. Otsuka, *Trends Glycosci. Glycotechnol.*, 2020, **32**, E63.
- 22 K. Shikinaka, M. Nakamura, R. R. Navarro and Y. Otsuka, *Green Chem.*, 2019, **21**, 498.
- 23 R. E. Neale, P. W. Barnes, T. M. Robson, P. J. Neale, C. E. Williamson, R. G. Zepp, S. R. Wilson, S. Madronich, A. L. Andrady, A. M. Heikkilä, G. H. Bernhard, A. F. Bals, P. J. Aucamp, A. T. Banaszak, J. F. Bornman, L. S. Bruckman, S. N. Byrne, B. Foereld, D.-P. Häder, L. M. Hollestein, W.-C. Hou, S. Hylander, M. A. K. Jansen, A. R. Klekociuk, J. B. Liley, J. Longstreth, R. M. Lucas, J. Martinez-Abaigar, K. McNeill, C. M. Olsen, K. K. Pandey, L. E. Rhodes, S. A. Robinson, K. C. Rose, T. Schikowski, K. R. Solomon, B. Sulzberger, J. E. Ukpebor, Q.-W. Wang, S.-Å. Wängberg, C. C. White, S. Yazar, A. R. Young, P. J. Young, L. Zhu and M. Zhu, *Photochem. Photobiol. Sci.*, 2021, **20**, 1.
- 24 I. Ohshima and A. Kikuhata, *US Pat.* 5763345, 1998.
- 25 J. Wang, T. Pan, J. Zhang, X. Xu, Q. Yin, J. Han and M. Wei, *RSC Adv.*, 2018, **8**, 21651.
- 26 R. Koppolu, J. Lahti, T. Abitbol, A. Swerin, J. Kuusipalo and M. Toivakka, *ACS Appl. Mater. Interfaces*, 2019, **11**, 11920.
- 27 F. Li, C. Zhang and Y. Weng, *ACS Omega*, 2020, **5**, 18675.
- 28 J. Li, S. Wang, L. Lai, P. Liu, H. Wu, J. Xu, S. J. Severtson and W.-J. Wang, *Carbon*, 2021, **172**, 31.
- 29 K. Kuraoka and K. Miki, *J. Ceram. Soc. Jpn.*, 2020, **128**(8), 573.